Rajanna, A., & Dettmann, C. P. (2018). Rateless Coded Adaptive Transmission in Cellular Networks: Role of Power Control. In *2018 IEEE International Conference on Communications (ICC 2018) : Proceedings of a meeting held 20-24 May 2018, Kansas City, Missouri, USA* (pp. 5446-5452). [8422964] Institute of Electrical and Electronics Engineers (IEEE). https://doi.org/10.1109/ICC.2018.8422964

Rateless Coded Adaptive Transmission in Cellular Networks: Role of Power Control

Amogh Rajanna and Carl P. Dettmann
School of Mathematics, University of Bristol, UK.
amogh.rajanna@ieee.org, carl.dettmann@bristol.ac.uk

***Abstract*—Adaptive transmission schemes are a key part of the radio design for 5G wireless channels. The paper studies the performance of two types of adaptive transmission schemes in cellular downlink. One is based on rateless codes with constant power and the other is fixed-rate codes in conjunction with power adaptation. Using a simple stochastic geometry model for cellular downlink, the focus is to understand the key impact of power adaptation in rateless and fixed-rate coded adaptive transmission. The performance of both rateless and fixed-rate coded adaptive transmission schemes are compared by evaluating the typical user rate and success probability achievable with the two schemes. Based on both theoretical analysis and simulation results, the paper clearly shows that rateless coding simplifies the role of power control in an adaptive transmission scheme.**

***Index Terms*—Adaptive Modulation and Coding, Rateless Codes, Power Adaptation, Fixed-Rate Codes, Adaptive Transmission, 5G Cellular Downlink.**

I. Introduction

Adaptive transmission techniques play a key role in the robust design of the radio access network architecture for 5G cellular networks. The intermittent/ fluctuating characteristics of the 5G wireless channel pose a bottleneck to the ultra-low latency and high reliability targeted goals of 5G networks and the applications they support. The ambitious goals of 5G networks will depend heavily on the performance of adaptive transmission techniques. The fundamental idea of adaptive transmission policy in the physical (PHY) layer is to ensure reliable transmission of bits between BS and user in the presence of varying channel conditions. This can be accomplished by choosing the best suitable code(s), coding rate, constellation sizes (modulation schemes) and also, by adapting the transmit power to channel conditions, i.e., power control. The aim is to achieve a constant E_b/N_0 for bit transmission over the wireless channel [1], [2]. Although adaptive transmission policies has been a well researched topic over the decades, there has been a renewed focus in this direction largely due to interesting developments in coding theory recently.

Rateless codes have the interesting property of being able to adapt both the code construction and the number of parity symbols to time-varying channel conditions. Although originally developed for the erasure channel in the last 10-15 years [3] [4], owing to the above properties, rateless codes have been investigated for the noisy channel, i.e., wireless communications too [5] [6]. From a coding theoretic perspective, the design and analysis of rateless codes over the noisy channel has been a much researched topic recently [7] [8] [9]. From a communication theory view, [10] studies the performance of rateless codes in the PHY layer of cellular downlink channel, comparing it to that of fixed-rate codes. The paper quantifies the enhancements on downlink channel due to a rateless coded PHY relative to fixed-rate codes.

The system model in [10] assumed constant power transmission. In this paper, we expand our understanding of how rateless codes form an integral part of adaptive transmission policy by studying their impact on power control. The focus is to investigate the performance of rateless codes and fixed-rate codes with transmit power adaptation. In order to understand whether power control has the same impact in both rateless and fixed-rate coded downlink systems, we compare the performance of fixed-rate coded downlink with truncated channel inversion or channel thresholding to that of rateless coding with constant power only. We show that fixed-rate coding with power adaptation performs good only in the low reliability/coverage regime whereas rateless coding with constant power does better in both low and high reliability regimes. Although power control has played a key role in fixed-rate coded 4G and prior cellular systems, our results show that rateless codes as part of the adaptive transmission policy relax/simplify the demands of power adaptation schemes.

II. System Model

A homogeneous Poisson point process (PPP) $\Phi = \{X_i\},\ i = 0, 1, 2, \cdots$ of intensity λ is used to model the locations of BSs in a cellular downlink setting. We make a simplifying assumption that each BS X_i transmits to one user in its Voronoi cell. The distance between BS X_i and its user, located uniformly random, at Y_i is D_i. We consider a fixed information transmission mode in which each BS transmits a K-bit packet to its user. At each BS, a physical layer rateless code is used to encode the K information bits. Each BS employs power control policy and its transmit power is γ_i.

The three elements that impair the wireless channel are small scale fading, path loss and interference. Channel has Rayleigh block fading, i.e., the K-bit packet is encoded and transmitted within a single coherence time. The packet transmission time of BS X_i to its user Y_i is denoted as T_i. Each K-bit packet transmission from a BS is subject to a delay constraint of N symbols (channel uses), i.e., $0 < T_i \leq N$. For a coherence time T_c and signal bandwidth W_c, the value of N is given as $N = T_c W_c$. At time $t \geq 0$, the

medium access control (MAC) state of BS X_i is given by $e_i(t) = 1\,(0 < t \leq T_i)$, where $1(\cdot)$ is the indicator function.

The received signal at user Y_i at time t is given by

$$y_i(t) = h_{ii} D_i^{-\alpha/2} x_i + \sum_{k \neq i} g_{ki} |X_k - Y_i|^{-\alpha/2} e_k(t) x_k + z_i,\ 0 < t \leq T_i, \tag{1}$$

where α is the path loss exponent, h_{ii} and g_{ki} are the fading coefficients. The 1^{st} term is the desired signal from BS X_i and the 2^{nd} term is the interference from BSs $\{X_k\}, k \neq i$. To facilitate an analytical study of the performance of an adaptive transmission policy based on rateless coding and power control, we consider two types of interference models in the cellular downlink. The two models are described below.

1) Time-varying Interference: In this model, the interference power at a user Y_i is function of time t. When the BS X_i is transmitting to its user Y_i, all other BSs interfere until they have completed their own K-bit packet transmission to their users, i.e., an interfering BS X_k will transmit for a duration of T_k channel uses from $t = 0$ and will subsequently turn OFF. For this case, the instantaneous interference power and SINR at user Y_i at time t are given by

$$I_i\,(t) = \sum_{k \neq i} \gamma_k |g_{ki}|^2 |X_k - Y_i|^{-\alpha} e_k(t) \tag{2}$$

and

$$\text{SINR}_i\,(t) = \frac{\gamma_i |h_{ii}|^2 D_i^{-\alpha}}{1 + I_i(t)}, \tag{3}$$

respectively. In (3), the noise power is normalized to 1.

The time-averaged interference at user Y_i up to time t is given by

$$\hat{I}_i(t) = \frac{1}{t} \int_0^t I_i(\tau)\, \mathrm{d}\tau. \tag{4}$$

Since every interfering BS transmits a K-bit packet to its user for T_k channel uses and becomes silent, the interference is monotonic w.r.t t, i.e., both $I_i(t)$ and $\hat{I}_i(t)$ are decreasing functions of t.

User Y_i employs a nearest-neighbor decoder based on CSIR only and performs minimum Euclidean distance decoding. The achievable rate $C_i(t)$ is given by [11]

$$C_i(t) = \log_2 \left(1 + \frac{\gamma_i |h_{ii}|^2 D_i^{-\alpha}}{1 + \hat{I}_i(t)}\right). \tag{5}$$

2) Constant Interference: In this model, we make a simplifying assumption that every interfering BS transmits to their user *continuously* without turning off. The MAC state of an interfering BS X_k at time t is thus given by $e_k(t) = 1,\ t \geq 0$. Hence, the interference power at the user Y_i does *not* change with time and is given by

$$I_i = \sum_{k \neq i} \gamma_k |g_{ki}|^2 |X_k - Y_i|^{-\alpha} \tag{6}$$

The achievable rate $C_i(t)$ in this model is given by

$$C_i(t) = \log_2 \left(1 + \frac{\gamma_i |h_{ii}|^2 D_i^{-\alpha}}{1 + I_i}\right). \tag{7}$$

The remainder of the discussion presented in this section applies to both the above interference models. Based on (5) and (7), the time to decode K information bits and thus, the packet transmission time T_i are given as

$$\hat{T}_i = \min\{t : K < t \cdot C_i(t)\} \tag{8}$$

$$T_i = \min(N, \hat{T}_i). \tag{9}$$

The distribution of the packet transmission time T_i in (9) is necessary to characterize the performance of an adaptive transmission policy using physical layer rateless codes and power control in a cellular network.

III. Typical User Analysis

To study the distribution of the packet transmission time, consider the typical user located at the origin. To characterize the complementary CDF (CCDF) of the packet transmission time T, we first note that the CCDFs of T and $\hat{T}$ are related as

$$\mathbb{P}\,(T > t) = \begin{cases} \mathbb{P}(\hat{T} > t) & t < N \\ 0 & t \geq N. \end{cases} \tag{10}$$

Next consider the below two events for the constant interference case,

$$\mathcal{E}_1(t) : \hat{T} > t$$

$$\mathcal{E}_2(t) : \frac{K}{t} \geq \log_2 \left(1 + \frac{\gamma |h|^2 D^{-\alpha}}{1 + I}\right), \tag{11}$$

where in (11), γ is the transmit power which depends on $|h|^2$ and I is the constant interference at origin given by

$$I = \sum_{k \neq 0} \gamma_k |g_k|^2 |X_k|^{-\alpha}. \tag{12}$$

Based on standard information theoretic results, a key observation is that for a given t, the event $\mathcal{E}_1(t)$ is true if and only if $\mathcal{E}_2(t)$ holds true. Thus

$$\mathbb{P}(\hat{T} > t) = \mathbb{P}\left(\frac{K}{t} \geq \log_2 \left(1 + \frac{\gamma |h|^2 D^{-\alpha}}{1 + I}\right)\right) \tag{13}$$

$$= \mathbb{P}\left(\frac{\gamma |h|^2 D^{-\alpha}}{1 + I} \leq \theta_t\right), \tag{14}$$

where $\theta_t = 2^{K/t} - 1$. Assuming a high enough BS density λ, we ignore the noise term for the remainder of the paper. For later use, define $\mathbf{P}_{ci} = 1 - \mathbb{P}(\hat{T} > t)$.

Under the time-varying interference case, the CCDF of $\hat{T}$ is given by

$$\mathbb{P}(\hat{T} > t) = \mathbb{P}\left(\frac{\gamma |h|^2 D^{-\alpha}}{\hat{I}(t)} \leq \theta_t\right), \tag{15}$$

where $\hat{I}(t)$ is the average interference up to time t at the typical user and is obtained from (4):

$$\hat{I}(t) = \sum_{k \neq 0} \gamma_k |g_k|^2 |X_k|^{-\alpha} \eta_k(t) \tag{16}$$

$$\eta_k(t) = \frac{1}{t} \int_0^t e_k(\tau)\, \mathrm{d}\tau = \min\left(1, T_k/t\right). \tag{17}$$

The marks $\eta_k(t)$ are correlated for different k. Define $\mathbf{P}_{vi} = 1 - \mathbb{P}(\hat{T} > t)$ for the time-varying interference case.

For the K-bit packet transmission to the typical user, the performance of the adaptive transmission policy is quantified through the success probability and rate of transmission. The success probability and rate of the typical user are defined as

$$p_{\rm s}(N) \triangleq 1 - \mathbb{P}(\hat{T} > N) \tag{18}$$

$$R_N \triangleq \frac{K p_{\rm s}(N)}{\mathbb{E}\left[T\right]} = \frac{K p_{\rm s}(N)}{\int_0^N \mathbb{P}(\hat{T} > t)\,{\rm d}t}. \tag{19}$$

Note that as per (9), T is a truncated version of $\hat{T}$ at N. A result for the success probabilities $\mathbf{P}_{ci}$ and $\mathbf{P}_{vi}$ appears below.

Proposition 1. *The success probability of K-bit packet transmission under the time-varying interference case is lower bounded by the success probability under the constant interference case*

$$\mathbf{P}_{ci} \leq \mathbf{P}_{vi}. \tag{20}$$

Proof: The proof follows directly from (14) and (15).

$$\mathbf{P}_{ci} = \mathbb{P}\left(\frac{\gamma|h|^2 D^{-\alpha}}{I} \geq \theta_t\right) \leq \mathbb{P}\left(\frac{\gamma|h|^2 D^{-\alpha}}{\hat{I}(t)} \geq \theta_t\right) = \mathbf{P}_{vi},$$

due to the fact that $I \geq \hat{I}(t)$ since $\eta_k(t) \leq 1$ in (16). ■

IV. Network Performance

In this section, we outline a methodology to compare the performance of three adaptive transmission strategies. For forward error correction (FEC), we consider two scenarios. In one scenario, the cellular network employs rateless codes for FEC while in the second scenario, conventional fixed-rate codes are used for FEC.

When the cellular network uses fixed rate codes for FEC, each BS encodes a K-bit information packet using a fixed rate code, e.g., an LDPC code, turbo code or Reed Solomon code and transmits the entire codeword of N parity symbols. The user receives the N parity symbols over the downlink channel and tries to decode the information packet using the BCJR or Viterbi algorithm. Based on instantaneous channel conditions, the single decoding attempt can be a success or not.

When the cellular network uses rateless codes for FEC, each BS encodes a K-bit packet using a variable length code, e.g., a Raptor code or a LT-concatenated code [5] (LT is Luby Transform) with degree distributions optimized for the noisy channel and also, being adaptive to the channel variations. The parity symbols are incrementally generated and transmitted until K bits are decoded at the user or the maximum number of parity symbols N is reached. The user performs multiple decoding attempts to decode the information packet using the Belief Propogation or Sum-Product algorithm. An outage occurs if the K bits are not decoded within N parity symbols.

In an adaptive transmission, the code type/rate, symbol power and modulation size can be made adaptive to channel conditions to ensure reliable transmission of bits. In this paper though, we limit the adaptation only to code type/rate and symbol power. Rateless codes have robust adaptivity to channel variations whereas fixed-rate codes do not have the same adaptivity to the channel (see [10] for more discussion). Hence for a decent (fair) choice of adaptive transmission schemes, we combine rateless codes with constant power and fixed-rate codes with power adaptation. Below we discuss three adaptive transmission policies and quantify their performance on the cellular downlink channel.

A. Rateless Coding with Constant Power

In the first adaptive transmission scheme we consider, the rateless codes are used for FEC and the transmit power is constant, i.e., no power adaptation. Based on (18) and (19), the success probability and rate of K-bit packet transmission can be obtained from the CCDF of the packet transmission time. From [10], the CCDF of the packet transmission time under the constant interference model for cellular downlink is given by

$$\mathbb{P}(\hat{T} > t) = 1 - \frac{1}{{}_2F_1\left([1, -\delta]\,; 1-\delta; -\theta_t\right)} \equiv P_{\rm c}(t), \tag{21}$$

where $\delta = 2/\alpha$ and ${}_2F_1\left([a,b]; c; z\right)$ is the Gauss hypergeometric function. Define $\theta = 2^{K/N} - 1$. The success probability $p_{\rm s}(N)$ can be written as

$$p_{\rm s}(N) = \frac{1}{{}_2F_1\left([1, -\delta]\,; 1-\delta; -\theta\right)}. \tag{22}$$

The rate R_N can be obtained based on (19) and (21) as

$$R_N = \frac{K p_{\rm s}(N)}{\int_0^N P_{\rm c}(t)\,{\rm d}t}. \tag{23}$$

Under the time-varying interference model, the CCDF of the packet transmission time given in (15) does not admit an explicit expression due to the correlated marks in $\hat{I}(t)$. In [10], an independent thinning model approximation is proposed to study the time-varying interference $\hat{I}(t)$ in (16) where in the correlated marks T_k are replaced by i.i.d. $\bar{T}_k$. From [10], an upper bound on the CCDF of the packet transmission time under the independent thinning approximation is given by

$$\mathbb{P}(\hat{T} > t) \leq \underbrace{1 - \frac{1}{{}_2F_1\left([1, -\delta]\,; 1-\delta; -\theta_t \min\left(1, \mu/t\right)\right)}}_{P_{\rm v}(t)} \tag{24}$$

$$\mu = \int_0^N \left(1 - {}_2F_1\left([1, \delta]\,; -\theta_t\right)\right)\,{\rm d}t, \tag{25}$$

where $\mu = \mathbb{E}[\bar{T}]$ is the expected packet transmission time of an interferer. (Details are omitted due to space limitations, please see [10].)

The $p_{\rm s}(N)$ under the independent thinning model is bounded as

$$\tilde{p}_{\rm s}(N) \geq \frac{1}{{}_2F_1\left([1, -\delta]\,; 1-\delta; -\theta\mu/N\right)}. \tag{26}$$

The rate R_N can be bounded based on (19) and (24) as

$$\tilde{R}_N \geq \frac{K \tilde{p}_{\rm s}(N)}{\int_0^N P_{\rm v}(t)\,{\rm d}t}. \tag{27}$$

When rateless codes are used for FEC, the typical user with constant interference can be interpreted as a user experiencing the worst type of interferer activity in a practical cellular network. Hence, $p_{\rm s}(N)$ and R_N in (22) and (23) for constant interference can be interpreted as a lower bound for the coverage and rate of a practical user in cellular downlink. In a similar way, $\tilde{p}_{\rm s}(N)$ and $\tilde{R}_N$ in (26) and (27) for time-varying interference can be interpreted as an upper bound for the rate of a practical user. Rateless coding is able to adapt to changing interference conditions and provide different rates, whereas fixed-rate coding settles for the low rate corresponding to transmitting N parity symbols for all types of users.

B. Fixed-Rate Coding with Channel Thresholding

In the second adaptive transmission scheme, the fixed-rate codes are used for FEC and a simple thresholding scheme is used for power adaptation. The power control scheme we consider is channel thresholding, in which the BS transmits with constant power ρ only if the channel gain $|h|^2$ exceeds a threshold β and declares an outage otherwise. Mathematically, the transmit power from BS to the typical user is given by

$$\gamma = \begin{cases} \rho, & |h|^2 \geq \beta \\ 0, & |h|^2 < \beta. \end{cases} \tag{28}$$

For fixed-rate coding, the packet transmission time of every BS is fixed to N channel uses and hence, interference is time-invariant as given in (12). The success probability and rate of the typical user are defined as

$$p_{\rm s}(N) \triangleq \mathbb{P}\left(\text{SIR} > \theta\right) = \mathbb{P}\left(\frac{\gamma |h|^2 D^{-\alpha}}{I} > \theta\right) \tag{29}$$

$$R_N \triangleq \frac{K}{N}\, p_{\rm s}(N). \tag{30}$$

Theorem 1. *The success probability $p_{\rm s}(N)$ in a cellular downlink employing fixed-rate coding and channel thresholding for adaptive transmission is given by*

$$p_{\rm s}(N) \approx \mathcal{F}(\theta) + \mathcal{F}(\theta/\beta)\left[e^{-\beta} - \mathcal{F}(\theta)\right] \tag{31}$$

$$\mathcal{F}(\theta) = \frac{e^{\beta}}{e^{\beta} - 1 + {}_2F_1\left([1, -\delta]\,; 1-\delta; -\theta\right)}. \tag{32}$$

The rate R_N can be obtained based on (30) and (31).

Proof: Refer to Appendix A. ∎

C. Fixed-Rate Coding with Truncated Channel Inversion

In the third adaptive transmission scheme, the FEC is done by using fixed-rate codes and the transmit power is adapted based on the value of channel gain $|h|^2$. The power control scheme we consider is truncated channel inversion, i.e., only if the channel gain $|h|^2$ exceeds a threshold β, adapt the power to invert the channel gain. Mathematically, the transmit power from BS to the typical user is given by

$$\gamma = \begin{cases} \rho/|h|^2, & |h|^2 \geq \beta \\ 0, & |h|^2 < \beta. \end{cases} \tag{33}$$

Theorem 2. *The success probability $p_{\rm s}(N)$ in a cellular downlink employing fixed-rate coding and truncated channel inversion for adaptive transmission is given by*

$$p_{\rm s}(N) \approx \frac{1}{1+G(\theta)}\, e^{-\beta} \tag{34}$$

$$G(\theta) = \theta^{\delta} \int_0^{\theta} \frac{\delta}{y^{\delta}}\, e^{y} E_1\left(\beta + y\right) \mathrm{d}y,$$

where $E_1(x) = \int_x^{\infty} e^{-t}/t \;\mathrm{d}t$ is the exponential integral function. The rate R_N can be obtained based on (30) and (34).

Proof: The proof appears in Appendix B. ∎

The second term in the RHS of (34) represents the loss due to channel truncation while the first term contains the gain due to truncated channel inversion. The adaptive transmission schemes are compared by evaluating the expressions for $p_{\rm s}(N)$ and R_N developed in this section.

V. Numerical Results

In this section, we present numerical results that illustrate the performance benefits of the adaptive transmission policies studied in the paper. The numerical results provide the performance of the typical user, which is the spatial average of all users performance in the network. For the simulation, the cellular network was realized on a square of side 60 with wrap around edges. The BS PPP intensity is $\lambda = 1$. The information packet size is $K = 75$ bits. The cellular network performance was evaluated for varying channel threshold β and delay constraint N. CI and TvI correspond to the constant and time-varying interference models described in Section II, respectively. The simulation curve corresponds to the cellular network simulation as per the time-varying interference model described in (2)-(9).

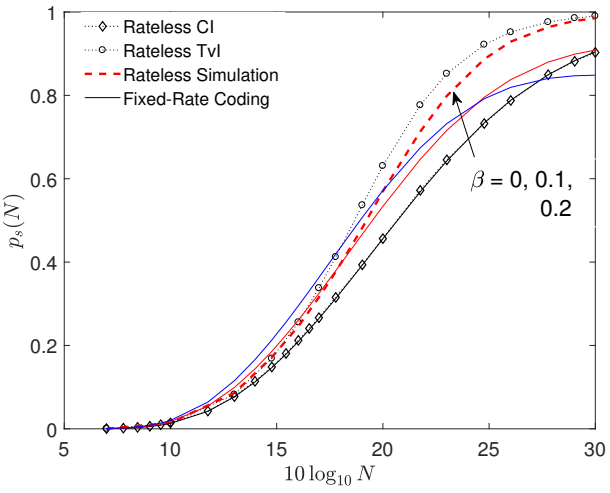

Fig. 1. Success probability $p_{\rm s}(N)$ as a function of the delay constraint N in a cellular network with $\lambda = 1$ at $\alpha = 3$ for both rateless coding and fixed-rate coding with channel thresholding based on (22), (26), (29) and (31) respectively. The solid curves correspond to fixed-rate coding with varying β.

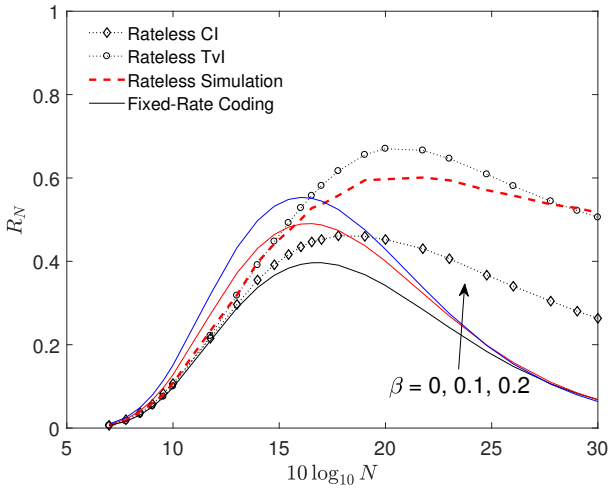

Fig. 2. The typical user rate R_N as a function of N in a cellular network with $\lambda = 1$ at $\alpha = 3$. For fixed-rate coding, the rate is based on (29), (30) and (31). For rateless coding, the rate is obtained from (23) and (27). The solid curves correspond to fixed-rate coding with varying β.

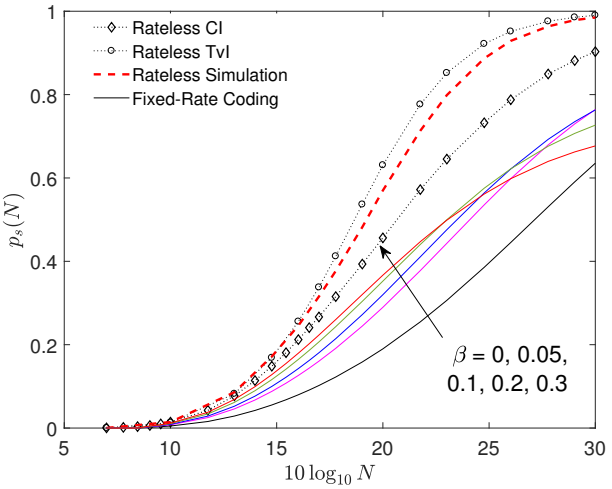

Fig. 3. Success probability $p_{\rm s}(N)$ as a function of the delay constraint N in a cellular network with $\lambda = 1$ at $\alpha = 3$. For fixed-rate coding with truncated channel inversion, the curves are based on (53) and (34). The solid curves correspond to fixed-rate coding with varying β.

Channel thresholding as a power adaptation scheme has both cost and benefit associated with it. The benefit is that it reduces the interference for the typical user. The cost being that the serving BS does not transmit to the user all the time, i.e., only when the channel gain exceeds the threshold. In Figs. 1 and 2, the success probability $p_{\rm s}(N)$ and rate R_N are plotted as a function of the delay constraint N for both rateless coding with constant power and fixed-rate coding with channel thresholding at $\alpha = 3$ and varying threshold β. In the high coverage regime, i.e., for large N, the cost of not transmitting to the user all the time becomes dominant relative to the benefit and thus, makes power adaptation inefficient. Hence for this regime, power adaptation along with fixed-rate coding has no advantages. Rateless coding with constant power transmission being adaptive to channel conditions, supplies only the necessary number of parity symbols to decode K bits achieving substantially higher throughput for both the interference models of Section II and hence is the preferred adaptive scheme in this regime.

In the low coverage (or high spectral efficiency/rate) regime, the benefit of channel thresholding, i.e., reduced interference allows the BS to transmit K bits to the user in favorable channel conditions. This benefit offsets the cost of power adaptation. So fixed-rate coding along with channel thresholding is useful in the low coverage regime. Rateless coding with no power adaptation still exhibits good performance due to the fact that expected packet time (parity symbols) is $\mathbb{E}[T]$ unlike non-adaptive fixed-rate coding which always transmits N parity symbols. The upper bound curve with time-varying interference has performance better than that of fixed-rate coding with power control over a wide range of N.

The benefit when channel inversion is used as a power adaptation scheme is that the fading from desired BS to user is compensated for. On the other hand, since the transmit

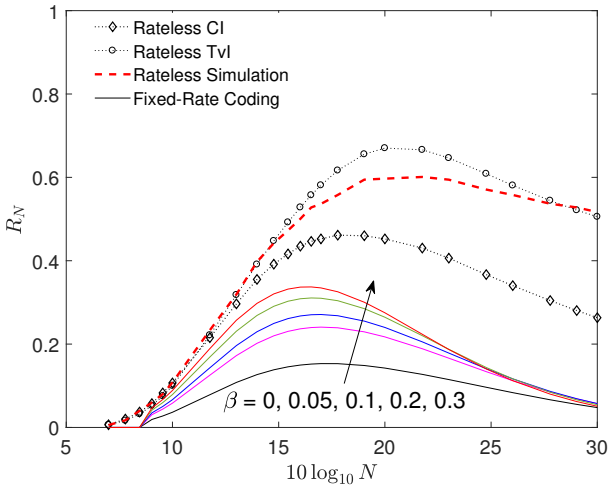

Fig. 4. The typical user rate R_N as a function of N in a cellular network with $\lambda = 1$ at $\alpha = 3$. For fixed-rate coding with truncated channel inversion, the rate is based on (30), (53) and (34).

power of interferers is also inversely proportional to Rayleigh fading, the total interference power at the typical user blows up. The increased interference at the user is the cost of channel inversion. Due to this cost, the thresholding policy $|h|^2 \geq \beta$ will be more useful in the case of channel inversion. Figs. 3 and 4 show plots of $p_{\rm s}(N)$ and R_N for both rateless coding with constant power and fixed-rate coding with truncated channel inversion for varying β. We observe that $\beta = 0.05$ provides a substantial increase in both $p_{\rm s}(N)$ and R_N relative to $\beta = 0$. (Similar behavior is observed for $\beta = 0.1$). For higher values of β in Figs. 3 and 4, we observe the same effect as in the case of channel thresholding, i.e., for large N the performance with a higher value of β is less than that

with a lower value of β (around 0.05). The thresholding policy is more beneficial in channel inversion compared to constant power transmission.

System Design Implications: From Figs. 3 and 4, we observe that for $N = 100$ rateless coding achieves a $p_{\rm s}(N)$ from 0.46 to 0.63 and for $N = 300$, 0.73 to 0.92 performance is achieved. On the other hand, for fixed-rate coding with truncated channel inversion, a very good $p_{\rm s}(N)$ can be obtained at $N = 100$ by choosing $\beta \geq 0.3$. At $N = 300$, a smaller value of β around 0.05 needs to be selected to get a decent performance. Hence for power control, the value of β needs to be optimized for N. Thus, to achieve a desired performance of $p_{\rm s}(N)$ and R_N, a fixed-rate coded system has to use channel inversion and thresholding along with a optimal $\beta^*(N)$ and this incurs a significant implementation (system) complexity relative to rateless coding with constant power transmission. For a K-bit packet transmission, rateless coding with no power control can achieve good E_b/N_0 for K bits with a higher probability, and a higher rate of transmission relative to fixed-rate coding with power adaptation.

VI. Conclusion

In this paper, we study three adaptive transmission schemes with the goal of achieving good E_b/N_0 for reliability over the wireless channel. For simplicity, we consider a cellular downlink with stochastic geometry model for BS locations and Rayleigh fading. We compare the performance of rateless coding with constant power to that of fixed-rate coding with power adaptation such as channel thresholding and truncated channel inversion. For fixed K-bit information transmission mode, it is shown that rateless coding with constant power performs much better relative to fixed-rate codes with power control in the moderate to high coverage regime. In the low coverage regime, the performance of the latter can be made as good as rateless codes by sophisticated choice of channel threshold β with added system complexity.

Acknowledgement

This work was supported by the EPSRC grant number EP/N002458/1 for the project *Spatially Embedded Networks*.

Appendix A
Proof of Theorem 1

First, the distribution of SIR in (29) is derived. Define an event $\mathcal{A} : |h|^2 \geq \beta$. Then for $\theta > 0$, the CCDF is given by

$$\mathbb{P}\left(\text{SIR} > \theta\right) = \mathbb{P}\left(\text{SIR} > \theta, \mathcal{A}\right) + \mathbb{P}\left(\text{SIR} > \theta, \bar{\mathcal{A}}\right) \tag{35}$$

$$\stackrel{(a)}{=} \underbrace{\mathbb{P}\Big(\frac{\rho|h|^2 D^{-\alpha}}{I} > \theta \mid \mathcal{A}\Big)}_{P_1(\theta)} \mathbb{P}(\mathcal{A}), \tag{36}$$

where (a) follows since the $2^{\rm nd}$ term in (35) has zero probability. To evaluate $P_1(\theta)$ in (36), the conditional CCDF of $|h|^2$ is given by

$$\mathbb{P}\left(|h|^2 > x \mid |h|^2 \geq \beta\right) = \begin{cases} e^{-x}/e^{-\beta}, & x \geq \beta \\ 1, & x < \beta. \end{cases} \tag{37}$$

Using (37), the probability $P_1(\theta)$ is expressed as

$$P_1(\theta) = \begin{cases} \mathbb{E}\left[e^{-\theta D^\alpha I/\rho}\right]/e^{-\beta}, & \theta D^\alpha I/\rho \geq \beta \\ 1, & \theta D^\alpha I/\rho < \beta. \end{cases} \tag{38}$$

Using $P_1(\theta)$ from (38) and $\mathbb{P}\left(\mathcal{A}\right) = e^{-\beta}$ in (36), we get

$$\begin{aligned} \mathbb{P}\left(\text{SIR} > \theta\right) &= \mathbb{E}\left[e^{-\theta D^\alpha I/\rho}\right] \mathbb{P}\left(\theta D^\alpha I/\rho > \beta\right) + \\ &\quad \mathbb{P}\left(\theta D^\alpha I/\rho < \beta\right) e^{-\beta} \\ &= \mathbb{E}\left[e^{-\theta D^\alpha I/\rho}\right] + \mathbb{P}\left(\theta D^\alpha I/\rho < \beta\right) \\ &\quad \left(e^{-\beta} - \mathbb{E}\left[e^{-\theta D^\alpha I/\rho}\right]\right) \end{aligned} \tag{39}$$

$$\mathbb{E}\left[e^{-\theta D^\alpha I/\rho}\right] \stackrel{(a)}{=} \mathbb{E}\left[\mathcal{L}_I\left(\theta D^\alpha/\rho\right)\right], \tag{40}$$

where (a) follows by taking the $\mathbb{E}[\cdot]$ operation w.r.t I by conditioning on D and $\mathcal{L}_I(s) = \mathbb{E}\left[e^{-sI}\right]$ is the Laplace transform of interference I by conditioning on D. Below we obtain an expression for $\mathcal{L}_I(\cdot)$. Note that in the expression for I in (12), γ_k is the transmit power from BS X_k to its user Y_k and follows the same policy as (28).

$$\begin{aligned} \mathcal{L}_I(s) &= \exp\left(-\pi\lambda \mathbb{E}_{\gamma,g}\left[\int_D^\infty \left(1 - e^{-s\gamma|g|^2 v^{-\alpha}}\right) \mathrm{d}v^2\right]\right) \\ &= \exp\left(-\pi\lambda \int_D^\infty \left(1 - \mathbb{E}\left[e^{-sv^{-\alpha}\gamma|g|^2}\right]\right) \mathrm{d}v^2\right). \end{aligned} \tag{41}$$

To evaluate the $\mathbb{E}\left[\cdot\right]$ in (41), let $c = sv^{-\alpha}$. Then

$$\mathbb{E}\left[e^{-c\gamma|g|^2}\right] = \sum_{\mathcal{A},\bar{\mathcal{A}}} \mathbb{E}\left[e^{-c\gamma|g|^2} \mid i\right] \mathbb{P}\left(i\right) \tag{42}$$

$$\begin{aligned} &= \mathbb{E}\left[e^{-c\rho|g|^2}\right] \mathbb{P}\left(\mathcal{A}\right) + \mathbb{P}\left(\bar{\mathcal{A}}\right) \\ &\stackrel{(a)}{=} 1 - e^{-\beta}\left(1 - \mathbb{E}\left[e^{-c\rho|g|^2}\right]\right), \end{aligned} \tag{43}$$

where (a) follows since $\mathbb{P}\left(\mathcal{A}\right) = e^{-\beta}$. Using (43), we can write (41) as

$$\mathcal{L}_I(s) = \exp\left(-\pi\lambda \int_D^\infty \left(1 - \mathbb{E}\left[e^{-sv^{-\alpha}\rho|g|^2}\right]\right) \mathrm{d}v^2 e^{-\beta}\right). \tag{44}$$

The exponent in (44), except for the term $e^{-\beta}$ is identical to the one which is obtained when BSs use constant transmission power [10]. The $e^{-\beta}$ factor is due to channel thresholding. Using $\mathcal{L}_I(s)$ for the constant power transmission case from [10] and substituting $s = \theta D^\alpha/\rho$, we get

$$\mathcal{L}_I(\theta D^\alpha/\rho) = \exp\left(-\pi\lambda D^2 H(\theta) e^{-\beta}\right) \tag{45}$$

$$H(\theta) = \frac{\theta\delta}{1-\delta}\ {}_2F_1\left([1, 1-\delta]; 2-\delta; -\theta\right). \tag{46}$$

Taking $\mathbb{E}\left[\cdot\right]$ of (45) w.r.t $D \sim$ Rayleigh $(1/\sqrt{2\pi\lambda})$, we get

$$\mathbb{E}\left[\mathcal{L}_I\left(\theta D^\alpha/\rho\right)\right] = \frac{1}{1 + H(\theta) e^{-\beta}} \equiv \mathcal{F}(\theta). \tag{47}$$

Based on (39) and (40), the CCDF of SIR is written as

$$\mathbb{P}(\text{SIR} > \theta) = \mathcal{F}(\theta) + \mathbb{P}\left(\frac{\theta D^\alpha I}{\rho} < \beta\right)\left[e^{-\beta} - \mathcal{F}(\theta)\right]. \tag{48}$$

Proposition 2. *The distribution of I in the RHS of (48) can be approximated as*

$$\mathbb{P}\left(\frac{\theta D^{\alpha} I}{\rho} < \beta\right) \approx \mathcal{F}(\theta/\beta). \tag{49}$$

Proof: The CDF of I in (49) can be rewritten as

$$\mathbb{P}\left(\frac{\theta D^{\alpha} I}{\rho} < \beta\right) = \mathbb{P}\left(\frac{\theta D^{\alpha} I}{\beta\rho} < \mathbb{E}\left[|h|^2\right]\right). \tag{50}$$

Consider the two RVs I and $|h|^2$ in (50). The RV I given in (12) is the dominant RV and mostly determines the scaling of the probability value. On the other hand, $|h|^2$ is the minor component since $|h|^2 \sim \text{Exp}(1)$ is a simple RV with $\mathbb{E}\left[|h|^2\right] = 1$ and PDF $= e^{-x},\ x \in [0, \infty)$. Hence, (50) can be approximated accurately as

$$\mathbb{P}\left(\frac{\theta D^{\alpha} I}{\beta\rho} < \mathbb{E}\left[|h|^2\right]\right) \approx \mathbb{P}\left(\frac{\theta D^{\alpha} I}{\beta\rho} < |h|^2\right) = \mathbb{E}\left[\exp\left(-\frac{\theta D^{\alpha} I}{\beta\rho}\right)\right] = \mathbb{E}\left[\mathcal{L}_I\left(\frac{\theta D^{\alpha}}{\beta\rho}\right)\right] \overset{(a)}{=} \mathcal{F}(\theta/\beta), \tag{51}$$

where (a) follows from (47). ∎

Using (51) in (48), the $p_{\text{s}}(N)$ can be approximated as in (31). The expressions for $\mathcal{F}(\theta)$ in (47) and (32) are related by the following hypergeometric identity

$$\frac{\delta}{1-\delta}\theta\ {}_2F_1\left([1, 1-\delta]; 2-\delta; -\theta\right) + 1 \equiv {}_2F_1\left([1, -\delta]; 1-\delta; -\theta\right). \tag{52}$$

Appendix B
Proof of Theorem 2

Below we characterize the distribution of the SIR in (29) based on the definition of γ in (33). Similar to (36), the CCDF of SIR can be written as

$$\mathbb{P}\left(\text{SIR} > \theta\right) = \mathbb{P}\Big(\frac{\rho D^{-\alpha}}{I} > \theta\Big)\mathbb{P}(\mathcal{A}) \tag{53}$$

(Note that $|h|^2$ does not appear in the RHS of (53)). Defining $P_1(\theta)$ similar to (36), we get

$$P_1(\theta) = \mathbb{P}\left(\frac{\rho D^{-\alpha}}{I} > \theta\right) = \mathbb{P}\left(\frac{\theta D^{\alpha} I}{\rho} < 1\right) \overset{(a)}{\approx} \mathbb{E}\left[\mathcal{L}_I\left(\theta D^{\alpha}/\rho\right)\right], \tag{54}$$

where (a) follows by using the same approximation as in Proposition 2 with $\beta = 1$. Now (53) can be written as

$$\mathbb{P}\left(\text{SIR} > \theta\right) \approx \mathbb{E}\left[\mathcal{L}_I\Big(\frac{\theta D^{\alpha}}{\rho}\Big)\right] e^{-\beta}. \tag{55}$$

To evaluate $\mathcal{L}_I(\cdot)$ in (54), we use (41) and (42). Applying the same steps from (42)-(43) for truncated channel inversion, we get

$$\mathbb{E}\left[e^{-c\gamma|g|^2}\right] = 1 - e^{-\beta}\left(1 - \mathbb{E}\left[e^{-c\rho|g|^2/|h|^2} \mid \mathcal{A}\right]\right) \tag{56}$$

$$= 1 - e^{-\beta}\left(1 - \mathbb{E}\left[\frac{1}{1 + c\rho/|h|^2} \mid \mathcal{A}\right]\right)$$

$$= 1 - e^{-\beta}\ \mathbb{E}\left[\frac{c\rho}{c\rho + |h|^2} \mid \mathcal{A}\right]. \tag{57}$$

Now plugging the value of c, (57) can be rewritten as

$$1 - \mathbb{E}\left[e^{-sv^{-\alpha}\gamma|g|^2}\right] = e^{-\beta}\ \mathbb{E}\left[\frac{1}{1 + |h|^2/s\rho v^{-\alpha}} \mid \mathcal{A}\right] \overset{(a)}{=} \int_{\beta}^{\infty} \frac{1}{1 + x/s\rho v^{-\alpha}} e^{-x}\,\mathrm{d}x, \tag{58}$$

where (a) follows from (37). Using (58) in (41) and substituting $s = \theta D^{\alpha}/\rho$, we get

$$\mathcal{L}_I\Big(\frac{\theta D^{\alpha}}{\rho}\Big) = \exp\left(-\pi\lambda \int_D^{\infty}\int_{\beta}^{\infty} \frac{e^{-x}}{1 + xv^{\alpha}/\theta D^{\alpha}}\,\mathrm{d}x\,\mathrm{d}v^2\right) \overset{(a)}{=} \exp\left(-\pi\lambda \int_{\theta}^{0}\int_{\beta}^{\infty} \frac{1}{1 + x/y} e^{-x}\,\mathrm{d}x\ D^2\theta^{\delta}\,\mathrm{d}y^{-\delta}\right)$$

$$= \exp\Big(-\pi\lambda D^2\ \underbrace{\theta^{\delta}\int_0^{\theta} \frac{\delta}{y^{\delta}}\int_{\beta}^{\infty} \frac{1}{x+y} e^{-x}\,\mathrm{d}x\,\mathrm{d}y}_{G(\theta)}\Big), \tag{59}$$

where (a) follows from the substitution $y = \theta(D/v)^{\alpha}$. Now using (59), we can evaluate the approximation in (55) as

$$\mathbb{P}\left(\text{SIR} > \theta\right) \approx \mathbb{E}\left[\exp\left(-\pi\lambda G(\theta) D^2\right)\right] e^{-\beta} = \frac{1}{1 + G(\theta)}\ e^{-\beta}, \tag{60}$$

since $D \sim$ Rayleigh $(1/\sqrt{2\pi\lambda})$. The function $G(\theta)$ in (59) can be written as

$$G(\theta) = \theta^{\delta}\int_0^{\theta} \frac{\delta}{y^{\delta}}\ e^{y} E_1\left(\beta + y\right)\,\mathrm{d}y. \tag{61}$$

From (60), the $p_{\text{s}}(N)$ can be expressed as in (34).

References

[1] A. J. Goldsmith and S.-G. Chua, "Variable-rate variable-power MQAM for fading channels," *IEEE Transactions on Communications*, vol. 45, no. 10, pp. 1218–1230, Oct 1997.

[2] ——, "Adaptive Coded Modulation for Fading Channels," *IEEE Transactions on Communications*, vol. 46, no. 5, pp. 595–602, May 1998.

[3] M. Luby, "LT Codes," in *Proc. of 43rd Annual IEEE Symp. Foundations of Computer Science*, Nov 2002, pp. 271–280.

[4] A. Shokrollahi, "Raptor Codes," *IEEE Transactions on Information Theory*, vol. 52, no. 6, pp. 2551–2567, June 2006.

[5] N. Bonello, Y. Yang, S. Sonia, and L. Hanzo, "Myths and Realities of Rateless Coding," *IEEE Communications Magazine*, no. 8, pp. 143–151, August 2011.

[6] E. Soljanin, N. Varnica, and P. Whiting, "Punctured vs. Rateless Codes for Hybrid ARQ," in *Proc. IEEE Info. Theory Workshop*, 2006, pp. 155–159.

[7] A. Kharel and L. Cao, "Improved Fountain Codes for BI-AWGN Channels," in *2017 IEEE Wireless Communications and Networking Conference (WCNC)*, Mar 2017, pp. 1–6.

[8] S. Tian, Y. Li, M. Shirvanimoghaddam, and B. Vucetic, "A Physical-Layer Rateless Code for Wireless Channels," *IEEE Transactions on Communications*, vol. 61, no. 6, pp. 2117–2127, June 2013.

[9] S. H. Kuo, H. C. Lee, Y. L. Ueng, and M. C. Lin, "A Construction of Physical-Layer Systematic Raptor Codes Based on Protographs," *IEEE Communications Letters*, vol. 19, no. 9, pp. 1476–1479, Sept 2015.

[10] A. Rajanna and M. Haenggi, "Enhanced Cellular Coverage and Throughput Using Rateless Codes," *IEEE Transactions on Communications*, vol. 65, no. 5, pp. 1899–1912, May 2017.

[11] A. Lapidoth, "Nearest neighbor decoding for additive non-Gaussian noise channels," *IEEE Transactions on Information Theory*, vol. 42, no. 5, pp. 1520 – 1529, Sept 1996.